J Elast (2013) 110:95–110
DOI 10.1007/s10659-012-9383-4

Optimum Young's Modulus of a Homogeneous Cylinder Energetically Equivalent to a Functionally Graded Cylinder

John Dryden · Romesh C. Batra

Received: 9 September 2011 / Published online: 4 April 2012

Abstract For a functionally graded (FG) circular cylinder loaded by uniform pressures on the inner and the outer surfaces and Young's modulus varying in the radial direction, we find lower and upper bounds for Young's modulus of the energetically equivalent homogeneous cylinder. That is, the strain energies of the FG and the homogeneous cylinders are equal to each other. For a typical power law variation of Young's modulus in the FG cylinder, it is shown that taking only two series terms, yields good values for bounds of the equivalent modulus. We also study two inverse problems. First, an investigation is made to find the radial variation of Young's modulus in the FG cylinder, having a constant Poisson's ratio, that gives the maximum value of the equivalent modulus. Second, the complementary problem of finding the radial variation of Poisson's ratio in the FG cylinder, having a constant stiffness, that gives the maximum value of the equivalent modulus, is considered. It is found that the spatial variation of the elastic properties, that maximizes the equivalent modulus, depends strongly upon the external loading on the cylinder.

Keywords Functionally graded material · Optimal stiffness variation · Circular cylinder

Mathematics Subject Classification 74B05 · 74E05

1 Introduction

A functionally graded material (FGM) is a non-homogeneous solid that is engineered so that the spatial variation of its physical properties produces better performance than is possible

J. Dryden (✉)
Department of Mechanical and Materials Engineering, University of Western Ontario, London, ON, N6A 5B9, Canada
e-mail: jdryden@uwo.ca

R.C. Batra
Department of Engineering Science and Mechanics, Virginia Polytechnic Institute and State University, Blacksburg, VA 24061, USA
e-mail: rbatra@vt.edu

from a monolithic solid. In the last several decades considerable research has been directed towards understanding the behavior of these solids. Here the deformation within circular cylinders is of interest and the analysis of homogeneous pressurized cylinders is given in standard textbooks [1–4]. The analyses of FG circular cylinders in references [5–12] consider thermoelastic deformation, and references [13–32] investigate the elastic field caused by an applied surface traction. Most of this work, has dealt with finding the stress and strain when the spatial variation of the elastic properties is specified. It is useful, for the purpose of designing FGM components, to have a method of finding the elastic properties of an equivalent homogeneous solid that has the same overall properties as the FGM. In the case of composite solids with discrete phases, this problem has received considerable attention over the last few decades, see, for example, [33–38].

In this contribution, the axisymmetric deformation of a FG circular cylinder is considered where the elastic properties are allowed to vary only in the radial direction. If the spatial variation of Young's modulus and Poisson's ratio are specified, then their volume average can be found by integrating them over the volume. For given average values of these elastic properties, how does their spatial variation influence the equivalent stiffness? Specifically, for a given average value of Young's modulus, what is the spatial distribution that leads to the maximum possible value of the equivalent stiffness? Often, it is implicitly assumed that the average Young's modulus represents an upper bound on the equivalent stiffness, and as shown herein this is not always true.

2 General Comments

We study the plane strain quasi-static deformation of a FG circular cylinder of length L, having inner and outer radii, equal to a and b respectively. The cylinder is subjected to an internal pressure $P\mathcal{I}$ and an external pressure $P\mathcal{O}$ where $\mathcal{I}$ and $\mathcal{O}$ are dimensionless quantities representing the fractional pressures. We assume that the cylinder material can be regarded as isotropic having Young's modulus $\hat{\boldsymbol{E}}(r)$ and Poisson's ratio $\hat{\boldsymbol{\nu}}(r)$ where r is the radial coordinate of a point in cylindrical coordinates with the origin at the cylinder center. Since the loads, the cylinder geometry, and material properties are independent of angular and axial position it is reasonable to assume that the deformations are axisymmetric. Therefore, the tangential displacement is zero, and the radial displacement depends only upon the radius, i.e., $u = u(r)$. The conditions

$$\begin{aligned} \varepsilon_r &= \frac{du}{dr}, \\ \varepsilon_\theta &= \frac{u}{r}, \end{aligned} \tag{1}$$

relate the strain to the displacement. The length L is taken as being much bigger than the outer radius, so that $L \gg b$, and, therefore, plane strain deformation is considered. It is convenient to define the quantities

$$\begin{aligned} E &\equiv \frac{\hat{\boldsymbol{E}}}{1-\hat{\boldsymbol{\nu}}^2}, \\ \nu &\equiv \frac{\hat{\boldsymbol{\nu}}}{1-\hat{\boldsymbol{\nu}}}. \end{aligned} \tag{2}$$

For the sake of brevity, we subsequently refer to E and ν as Young's modulus and Poisson's ratio respectively, and for the plane strain condition considered here, Hooke's law is written as

$$\begin{aligned} \frac{du}{dr} &= \frac{\sigma_r - \nu\sigma_\theta}{E}, \\ \frac{u}{r} &= \frac{\sigma_\theta - \nu\sigma_r}{E}. \end{aligned} \tag{3}$$

To solve the pressurized cylinder problem, it is well known that mechanical equilibrium is maintained if the stress components are defined from a stress function Ψ so that

$$\sigma_r = -\frac{\Psi}{r}, \qquad \sigma_\theta = -\frac{d\Psi}{dr}. \tag{4}$$

This stress function must satisfy the following two boundary conditions:

$$\Psi(a) = aP\mathcal{I}, \qquad \Psi(b) = bP\mathcal{O}. \tag{5}$$

To find the function Ψ, an ordinary differential equation is formulated by forcing compatibility onto the two conditions for the displacement u given in (3).

We scale the radial coordinate with respect to the inner radius,

$$\rho = \frac{r}{a}, \tag{6}$$

and the dimensionless outer radius is $\beta = b/a > 1$. A dimensionless displacement $U = U(\rho)$ is defined by

$$u = \frac{PaU}{E_{av}}, \tag{7}$$

where

$$E_{av} \equiv \frac{2}{\beta^2 - 1}\int_1^\beta E(\rho)\rho\, d\rho, \tag{8}$$

is the volume average of E. One of the aims of this contribution is to investigate (for a given value of E_{av}) how the spatial variation of E influences the overall equivalent stiffness. A non-dimensional function $\mathtt{E} = \mathtt{E}(\rho)$ is defined so that the elastic stiffness is described by the following relation

$$E = E_{av}\,\mathtt{E}. \tag{9}$$

It then follows from (8) that $\mathtt{E}$ satisfies the condition

$$\int_1^\beta \mathtt{E}\rho\, d\rho = \frac{\beta^2 - 1}{2}, \tag{10}$$

which represents a constraint on the function $\mathtt{E}$. No restriction, other than $0 \le \nu \le 1$ is placed upon $\nu = \nu(\rho)$ at this stage.

Finally, a dimensionless stress function ψ is defined by the conditions

$$\sigma_r = -\frac{P\psi}{\rho}, \qquad \sigma_\theta = -P\psi', \tag{11}$$

where $\psi' \equiv d\psi/d\rho$. This stress function must satisfy the following two boundary conditions:

$$\psi(1) = \mathcal{I}, \qquad \psi(\beta) = \beta\mathcal{O}. \tag{12}$$

To ensure compatibility, this stress function must satisfy the differential equation

$$\left(\frac{\rho\psi' - \nu\psi}{\mathtt{E}}\right)' - \left(\frac{\psi/\rho - \nu\psi'}{\mathtt{E}}\right) = 0, \tag{13}$$

which is derived by combining (3), (7), (9), and (11).

3 Equivalent Homogeneous Solid

Our goal is to find Young's modulus, E_h, of an energetically equivalent homogeneous cylinder. So, consider a homogeneous equivalent solid having constant elastic stiffness E_h and constant Poisson's ratio. For this solid, $\mathtt{E} = 1$, and the solution to (13) is

$$\psi_0 = \left(\frac{\beta^2\mathcal{O} - \mathcal{I}}{\beta^2 - 1}\right)\rho + \left(\frac{\mathcal{I} - \mathcal{O}}{\beta^2 - 1}\right)\frac{\beta^2}{\rho}. \tag{14}$$

The strain energy density is given by $(\sigma_r^2 - 2\nu\sigma_r\sigma_\theta + \sigma_\theta^2)/2E$, and, after integrating over the volume, the strain energy is found to be

$$\mathcal{J}_h = \frac{2P^2\pi a^2 L G_h}{E_h}, \tag{15}$$

where the quantity G_h is written as

$$G_h = \frac{\mathcal{I}^2\{(\nu+1)\beta^2 - (\nu-1)\} - 4\beta^2\mathcal{I}\mathcal{O} - \mathcal{O}^2\beta^2\{(\nu-1)\beta^2 - (\nu+1)\}}{2(\beta^2-1)}. \tag{16}$$

So the expression for the strain energy $\mathcal{J}_h$ of a homogeneous cylinder is known.

4 Lower Bound for E_h

The strain energy of the FG cylinder is written as

$$\mathcal{J} = \frac{2P^2\pi a^2 L G}{E_{av}}, \tag{17}$$

where

$$G = \int_1^\beta J(\psi, \psi')\, d\rho, \tag{18}$$

and the integrand $J(\psi, \psi')$ is

$$J(\psi, \psi') = \frac{\rho}{2\mathtt{E}}\left(\frac{\psi^2}{\rho^2} - \frac{2\nu\psi\psi'}{\rho} + \psi'^2\right). \tag{19}$$

After integration by parts it follows that G can be written as

$$G = \frac{1}{2}\left[\frac{\psi(\rho\psi' - \nu\psi)}{\mathtt{E}}\right]_1^\beta - \frac{1}{2}\int_1^\beta \psi\left\{\left(\frac{\rho\psi' - \nu\psi}{\mathtt{E}}\right)' - \left(\frac{\psi/\rho - \nu\psi'}{\mathtt{E}}\right)\right\} d\rho. \tag{20}$$

The first term on the right hand side is evaluated at the boundaries, and the second term, which is an integral over the volume, vanishes if the Euler condition (13) is satisfied. Therefore, if the stress function is the exact solution, then the strain energy, $\mathcal{J}$, equals one-half the work done by the surface traction applied on the inner and outer surfaces of the cylinder. Furthermore, it is known that the strain energy attains its absolute minimum $\mathcal{J}_e$ if ψ satisfies the Euler equation. Thus, setting $\mathcal{J}_e = \mathcal{J}_h$ leads to the exact expression for E_h.

Since it is not always possible to obtain the exact solution an approximate expression, ψ_a, is used in (18) and $\mathcal{J}_a \geq \mathcal{J}_h$, so that $G_a/E_{av} \geq G_h/E_h$. This can be rewritten as

$$\frac{E_h}{E_{av}} \geq \frac{G_h}{G_a}, \tag{21}$$

and represents a lower bound for E_h. To construct this lower bound, an approximate stress function ψ_a needs to be found, and this approximate function must satisfy the boundary conditions $\psi_a(1) = \mathcal{I}$ and $\psi_a(\beta) = \beta\mathcal{O}$ as given in (12). With this in mind the stress function is approximated by the series

$$\psi \approx \psi_0 + \sum_{n=1}^{N} B_n \psi_n, \tag{22}$$

where ψ_0 is the solution for homogeneous cylinder and the functions ψ_n which account for the non-homogeneity are given by

$$\psi_n = \rho^{n-1}(\rho - 1)(\beta - \rho).$$

An approximation G_a for integral in (18) is then found in the form

$$G_a = \gamma_0 + \sum_{k=1}^{N} \gamma_k B_k + \sum_{i=1}^{N}\sum_{j=1}^{N} \gamma_{ij} B_i B_j, \tag{23}$$

where γ_0 is written as

$$\gamma_0 = \int_1^\beta \left\{\rho(1-\nu)\left(\frac{\beta^2\mathcal{O} - \mathcal{I}}{\beta^2 - 1}\right)^2 + (1+\nu)\left(\frac{\mathcal{I} - \mathcal{O}}{\beta^2 - 1}\right)^2 \frac{\beta^4}{\rho^3}\right\} \frac{d\rho}{\mathtt{E}},$$

and the other coefficients, γ_k and γ_{ij}, can be calculated. The coefficients B_j are found by solving the set of linear equations obtained from the conditions $\partial G/\partial B_m = 0$.

5 Upper Bound for E_h

An upper bound can be constructed by using the method proposed by Arthurs [39]. First, the quantity

$$-U \equiv \frac{\partial J}{\partial \psi'} = \frac{\rho\psi' - \nu\psi}{\mathtt{E}} \tag{24}$$

is defined, and, by comparison with (3) and (11), it is clear that U is the dimensionless displacement defined in (7). Solving for ψ' yields the result

$$\psi' = -\frac{\mathrm{E}U}{\rho} + \frac{\nu\psi}{\rho}. \tag{25}$$

The Legendre transform of J is written as $H = -U\psi' - J(\psi, \psi')$, and, using (19) and (25), it follows that

$$H = \frac{\mathrm{E}U^2}{2\rho} - \frac{\nu\psi U}{\rho} - \frac{1-\nu^2}{2\mathrm{E}\rho}\psi^2, \tag{26}$$

where $H = H(U, \psi)$ is known in terms of U and ψ. Following the standard treatment $U' = \partial H/\partial\psi$ leads to

$$U' = -\frac{1-\nu^2}{\mathrm{E}\rho}\psi - \nu\frac{U}{\rho}. \tag{27}$$

The function ψ can then be found as

$$\psi = -\frac{\mathrm{E}\rho}{1-\nu^2}\left\{U' + \nu\left(\frac{U}{\rho}\right)\right\}. \tag{28}$$

The quantity $J = -U\psi' - H$ is used in (18). The term $-U\psi'$ is integrated by parts, and after eliminating ψ the strain energy is found in terms of displacement

$$\mathcal{J} = \frac{2P^2\pi a^2 LF}{E_{av}},$$

where the functional F is

$$F = \mathcal{I}U(1) - \beta\mathcal{O}U(\beta) - \int_1^\beta I\bigl(U, U'\bigr)\,d\rho. \tag{29}$$

The quantity $I(U, U')$ is given by

$$I\bigl(U, U'\bigr) = \frac{\mathrm{E}\rho}{2(1-\nu^2)}\left\{U'^2 + 2\nu U'\left(\frac{U}{\rho}\right) + \left(\frac{U}{\rho}\right)^2\right\}. \tag{30}$$

The expression for F corresponds to the work done by external forces minus the strain energy. When F reaches its extremum, the work is twice the strain energy and this is essentially Clapeyron's theorem [2]. The case where $\nu = 1$ can be analyzed by substituting $U = B/\rho$ in (30) and performing a limiting process where $\nu \to 1$.

The Euler equation corresponding to the integrand given in (30) represents the condition for mechanical equilibrium and if U satisfies the Euler equation then $\mathcal{J}$ attains its maximum possible value $\mathcal{J}_e$. If an approximate expression U_a for the displacement is used, then $\mathcal{J}_a \leq \mathcal{J}_e = \mathcal{J}_h$. From this it follows that

$$\frac{E_h}{E_{av}} \leq \frac{G_h}{F_a},$$

and this represents an upper bound for the stiffness, E_h.

5.1 Approximate Solution

From consideration of the theory in variational calculus, it can be shown that (unlike the functional G in terms of ψ) all the requirements for F to reach a maximum are self-contained in the functional F, and, for this reason, no conditions are placed on an approximate form for the displacement. For the sake of simplicity the displacement is written as

$$U = A\rho + \frac{B}{\rho}. \tag{31}$$

With this form, there is no interaction energy between the components $A\rho$ and B/ρ so that the expression for I is written as

$$I\big(U, U'\big) = \frac{\mathrm{E}\rho}{(1-\nu^2)}\left\{A^2(1+\nu) + \frac{B^2(1-\nu)}{\rho^4}\right\}. \tag{32}$$

The approximate expression, F_a, found using (29) reduces to

$$\begin{aligned} F_a = &\left\{A\big(\mathcal{I} - \beta^2\mathcal{O}\big) - A^2\int_1^\beta \frac{\mathrm{E}\rho\, d\rho}{1-\nu}\right\} \\ &+ \left\{B(\mathcal{I} - \mathcal{O}) - B^2\int_1^\beta \frac{\mathrm{E}}{1+\nu}\frac{d\rho}{\rho^3}\right\}. \end{aligned} \tag{33}$$

The coefficients A and B are then adjusted to maximize F_a and this gives

$$\begin{aligned} A &= \frac{\mathcal{I} - \beta^2\mathcal{O}}{2}\left[\int_1^\beta \frac{\mathrm{E}\rho}{1-\nu}d\rho\right]^{-1}, \\ B &= \frac{\mathcal{I} - \mathcal{O}}{2}\left[\int_1^\beta \frac{\mathrm{E}}{1+\nu}\frac{d\rho}{\rho^3}\right]^{-1}. \end{aligned} \tag{34}$$

Using these values for A and B, the maximum value of F_a is found as

$$F_a = \left(\frac{\mathcal{I} - \beta^2\mathcal{O}}{2}\right)^2\left[\int_1^\beta \frac{\mathrm{E}\rho}{1-\nu}d\rho\right]^{-1} + \left(\frac{\mathcal{I} - \mathcal{O}}{2}\right)^2\left[\int_1^\beta \frac{\mathrm{E}}{1+\nu}\frac{d\rho}{\rho^3}\right]^{-1}. \tag{35}$$

As expected, in the case where the cylinder is subjected to hydrostatic stress, i.e., $\mathcal{I} = \mathcal{O}$, the strain energy vanishes for an incompressible solid for which $\nu = 1$.

6 Comparison Between Lower and Upper Bounds

The lower and upper bounds are compared against the exact solution which is readily accessible if Poisson's ratio is constant and the spatial variation of E is described by a power law

$$\mathrm{E}_k(\rho) = \frac{K}{\rho^{2k}}. \tag{36}$$

The subscript "k" indicates power law behavior. For the power law behavior of E given in (36), the stress function can be readily found by solving the Euler equation (13) and the solution that satisfies the boundary conditions in (12) is

$$\psi_k = \left(\frac{\mathcal{O}\beta - \mathcal{I}\beta^n}{\beta^p - \beta^n}\right)\rho^p + \left(\frac{\mathcal{I}\beta^p - \mathcal{O}\beta}{\beta^p - \beta^n}\right)\rho^n, \tag{37}$$

where the positive and negative characteristic roots are

$$p = -k + q,$$
$$n = -k - q,$$

and $q = \sqrt{1 + 2k\nu + k^2}$. The integral G defined in (18) can be calculated and is labeled $G = G_k$. It is convenient to define a parameter $m \equiv \ln\beta$ and G_k is then written as

$$G_k = \frac{\mathcal{I}^2 f - 2\mathcal{O}\mathcal{I}g + \mathcal{O}^2 h}{2K}. \tag{38}$$

The functions f, g, and h, which depend upon the material properties and the geometry, are written as

$$\begin{aligned} f &= q\,\mathrm{cth}\,mq + \nu + k, \\ g &= \exp\big[m(1+k)\big]\, q\,\mathrm{csch}\,mq, \\ h &= \exp\big[2m(1+k)\big]\,(q\,\mathrm{cth}\,mq - \nu - k), \end{aligned} \tag{39}$$

where $\mathrm{cth}\,x \equiv \cosh x/\sinh x$, $\mathrm{csch}\,x \equiv 1/\sinh x$. The constraint on $\mathtt{E}_k(\rho)$, given in (10), is satisfied if

$$K = \left(\frac{m(1-k)}{\exp[2m(1-k)] - 1}\right)\left(\frac{\exp[2m] - 1}{m}\right), \quad k \neq 1. \tag{40}$$

If $k = 1$, the expression for K is indeterminate, and l'Hôpital's rule can be used to find $K = (\exp[2m] - 1)/2m$. For a homogeneous solid $k = 0$, $K = 1$, $q = p = 1$, $n = -1$, and

$$G_0 = \frac{\mathcal{I}^2(\mathrm{cth}\,m + \nu) - 2\mathcal{O}\mathcal{I}\exp[m]\,\mathrm{csch}\,m + \mathcal{O}^2\exp[2m](\mathrm{cth}\,m - \nu)}{2}. \tag{41}$$

By comparison with (16) it can be confirmed that $G_0 = G_h$. The equivalent stiffness is then given by

$$\frac{E_h}{E_{av}} = \frac{G_0}{G_k}. \tag{42}$$

The lower and upper bounds, developed in Sects. 4 and 5 respectively, can be compared with this exact result for the stiffness ratio. It is also of interest to compare these results against the classical Voigt and Reuss bounds. According to Avseth et al. [38], the Voigt upper bound, E_V, and the Reuss lower bound E_R, (both of which were established early in the twentieth century) represent the simplest expressions for bounds. The bounds are $E_V \geq E_h \geq E_R$ where in this case E_V and E_R are found using the following expressions:

$$\begin{aligned} \frac{E_V}{E_{av}} &= \frac{2}{\beta^2 - 1}\int_1^\beta \mathtt{E}\rho\, d\rho \equiv 1, \\ \frac{E_{av}}{E_R} &= \frac{2}{\beta^2 - 1}\int_1^\beta \frac{\rho}{\mathtt{E}}\, d\rho. \end{aligned} \tag{43}$$

In the Voigt bound the strain is assumed to be constant, while in the Reuss bound the stress is assumed to be constant.

6.1 Numerical Results

To obtain some numerical results, typical, but arbitrary values are used: $\beta = 2$ ($m = \ln 2$); Poisson's ratio $\hat{\nu} = 1/3$ ($\nu = 1/2$); and in (36) the quantity $k = \pm 3/2$. The Reuss modulus, E_R, is an even function of k so the classical bounds are the same for $k = \pm 3/2$. Using (43) the Voigt and Reuss bounds are found as

$$1 \geq \frac{E_h}{E_{av}} \geq \frac{45}{62}. \tag{44}$$

Unlike the classical bounds, the bounds developed in Sects. 4 and 5, depend on the ratio of $\mathcal{I}$ to $\mathcal{O}$. With this in mind it is convenient to define a parameter t such that

$$\begin{aligned} \mathcal{I} &= \cos t, \\ \mathcal{O} &= \sin t, \end{aligned} \tag{45}$$

where $0 \leq t \leq 2\pi$. The dependence of the stiffness ratio E_h/E_{av} upon the ratio $\mathcal{I}/O$ can be found. For all possible ratios of $\mathcal{I}/\mathcal{O}$, the exact result given in (42) is compared with the lower and upper bounds. These bounds are found using only the leading term: the lower bound, given in (23), is found by setting $G_a = \gamma_0$; and, the upper bound is constructed using F_a given in (35). Figure 1(a) shows a graph of $\mathtt{E}$ versus ρ when $k = 3/2$, and Fig. 1(b) shows the dependence of E_h/E_{av} upon the parameter t. Similarly, Fig. 2(a) shows a graph of $\mathtt{E}$ versus ρ when $k = -3/2$, and Fig. 2(b) shows the dependence of E_h/E_{av} upon the parameter t. By taking 2 or 3 series terms, both the upper and lower bounds can be made to be virtually identical to the exact solution; this of course requires considerably more computational effort. The classical bounds, given in (44), are based upon either constant stress or strain and for a homogeneous solid this occurs only when $\mathcal{I} = \mathcal{O}$. Along this line the bounds presented here agree with the classical bounds. For other loading, i.e., $\mathcal{I} \neq \mathcal{O}$, the classical bounds are not generally valid as can be seen in both Figs. 1(b) and 2(b).

7 Tailoring the Stiffness when ν Is Constant

In practice the properties of FGMs vary gradually and if an admissible stress field is specified, then the function ψ can be found. The stiffness $\mathtt{E}$ required to produce this stress can be calculated from (13), and, if Poisson's ratio is constant, (13) can be rewritten as

$$\mathtt{E}'\big[\zeta + (1-\nu)\psi\rho\big] - \mathtt{E}\zeta' = 0, \tag{46}$$

where $\zeta = \rho^3(\psi/\rho)'$. The solution to this differential equation is

$$\mathtt{E} = \lambda \exp\left[\int \frac{\zeta' d\rho}{\zeta + (1-\nu)\rho\psi}\right], \tag{47}$$

where λ is a constant of integration. Except for the special case when $\nu = 1$, the integral in (47) is intractable and it must be solved numerically.

For design purposes it is attractive to find a distribution for $\mathtt{E}$ that is commensurate with a large value of the equivalent stiffness, and finding the function $\mathtt{E}$ that causes a specified

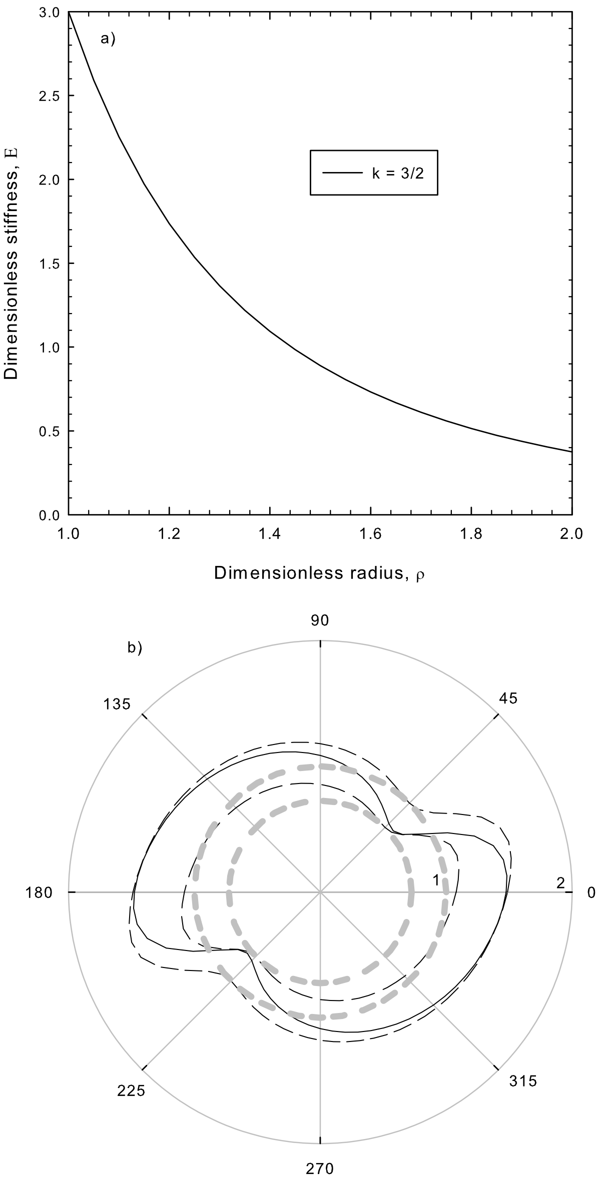

Fig. 1 (**a**) Variation with ρ of the dimensionless stiffness $\mathtt{E} = 3/\rho^3$ corresponding to $k = 3/2$; (**b**) Polar graph showing the behavior of E_h/E_{av} (the length from the origin to a point on the curve) versus the parameter t given in (45). The upper and lower bounds are shown by the *dashed lines*, while the exact solution is indicated by the solid line. Internal and external pressures correspond to $t = 0°$ and $90°$ respectively, and hydrostatic loading is represented by $t = 45°$. The *dashed gray circles*, having radii equal to 1 and $45/62$, represent the classical bounds given in (44). Along the line representing hydrostatic loading, $t = 45°$, the classical bounds agree with the bounds given here

stress field does not necessarily fulfill this aim. The strain energy $\mathcal{J}$ depends on the integral for G, which is given in (18), and can be written as

$$G = \frac{1}{2}\int_1^{\beta} \rho \left\{ \frac{\sigma^2}{\mathtt{E}} + \varepsilon^2(\mathtt{E} - 1) \right\} d\rho, \tag{48}$$

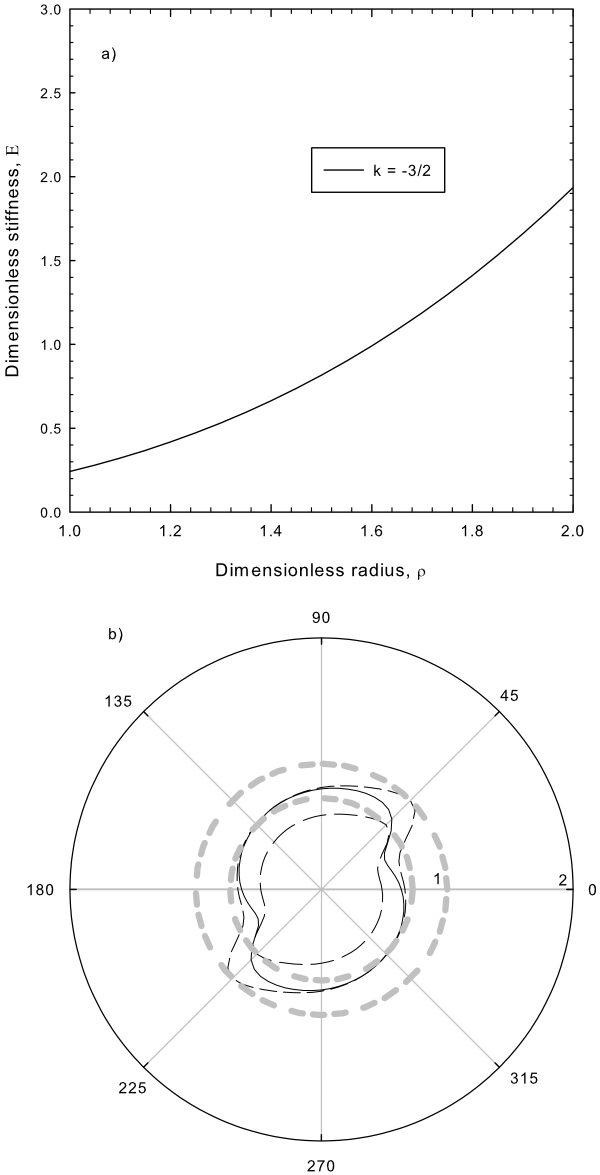

Fig. 2 (**a**) Variation with ρ of $\mathtt{E} = 15\rho^3/62$ corresponding to $k = -3/2$; (**b**) Polar graph showing the behavior of E_h/E_{av} (the length from the origin to a point on the curve) versus the load parameter t given in (45). The upper and lower bounds are shown by the *dashed lines*, while the exact solution is indicated by the *solid line*. Internal and external pressures correspond to $t = 0°$ and $90°$ respectively, and hydrostatic loading is represented by $t = 45°$. The *dashed gray circles*, having radii equal to 1 and $45/62$, represent the classical bounds given in (44). Along the line representing hydrostatic loading, $t = 45°$, the classical bounds agree with the bounds given here

where the term multiplied by the constant ε^2 represents the constraint upon $\mathtt{E}$. The dimensionless "stress" term σ is defined as

$$\sigma \equiv \sqrt{\frac{\psi^2}{\rho^2} - \frac{2\nu\psi\psi'}{\rho} + \psi'^2}. \tag{49}$$

If ψ is known then σ can be calculated and it can be shown that setting

$$\mathtt{E} = \frac{\sigma}{\varepsilon}, \tag{50}$$

minimizes the integral for G. Intuitively, it seems plausible that $\mathtt{E}$ should be large in regions where the stress σ is large if the overall stiffness is to be maximized. So the aim is to find ψ that minimizes G for a given $\mathtt{E}$, and also to find $\mathtt{E}$ that minimizes G for a given ψ. When $\mathtt{E}$ is readjusted then the stress function no longer satisfies the Euler equation, and an iterative process is required.

Alternatively, an approximation for the optimum overall stiffness can be found if the dimensionless stiffness is based on the power law, $\mathtt{E} = \mathtt{E}_k$, given in (36). The expression for $G = G_k$ is given in (38), and finding the value for k that minimizes G_k is roughly equivalent to specifying $\mathtt{E} \propto \sigma$. As shown subsequently, the value for k that minimizes G_k depends on the external loading. To begin, it is useful to consider the series expansion around $k = 0$ and the first two terms are

$$G_k = G_0 + \frac{(\mathcal{O} - \mathcal{I})^2}{2}\left\{\frac{(1+\nu)\exp[m](1 - m\,\mathrm{cth}\,m)}{\sinh m}\right\}k + O\big(k^2\big), \tag{51}$$

where $m = \ln\beta$. It is clear from this result that if the internal and external pressures are equal, i.e., $\mathcal{I} = \mathcal{O}$, the coefficient of k vanishes and G attains a minimum when $k = 0$. This corresponds to the stress function, $\psi_k = \mathcal{I}\rho$, and σ is constant so that condition in (50) is satisfied if $\mathtt{E} = 1$. Therefore, for constant stress, the maximum equivalent stiffness occurs when the modulus is constant. This can be illustrated in a simple way by considering a two-phase series model where the stress is constant. The volume fraction of phase 1 is ϕ, while E_1 and E_2 are the moduli of phases 1 and 2 respectively. The strain energy density is

$$\frac{\sigma^2}{2E_h} = \frac{1}{2}\left\{\frac{\sigma^2\phi}{E_1} + \frac{\sigma^2(1-\phi)}{E_2} + \varepsilon^2\big[\phi E_1 + (1-\phi)E_2 - E_{av}\big]\right\},$$

where the term multiplied by the Lagrange multiplier ε^2 represents the constraint upon the average stiffness. Setting the partial derivatives with respect to E_1 and E_2 equal to zero leads to the result that $E_1 = E_2$ and E is uniform.

For an internally pressurized cylinder, $\mathcal{O} = 0$, $G_k = \mathcal{I}^2 f/2K$, and there is no possibility that the stress is constant. Near $k = 0$ it follows from (51) that $dG_k/dk < 0$. By considering the behavior of G_k for large values of k, it is found that this derivative monotonically increases and approaches zero as k becomes large. The optimum stiffness is achieved when $\mathtt{E}$ is concentrated near the inner surface. The effective stiffness is

$$\frac{E_h}{E_{av}} \sim \frac{(\beta^2+1) + \nu(\beta^2-1)}{2}, \tag{52}$$

and this represents the limit as k becomes very large.

For an externally pressurized cylinder, $\mathcal{I} = 0$ and $G_k = \mathcal{O}^2 h/2K$. Intuitively, it is expected that when $\beta \gg 1$, then the stiffness will adjust itself so that $k \to 0$ and the stress state over most of the volume corresponds to uniform stress. On the other hand, when β is comparable with unity, the values of k become large and $G_k \propto \exp[2mk]/k^2$. This is minimized when

$$k = \frac{1}{m}.$$

The effective stiffness is then approximately given by

$$\frac{E_h}{E_{av}} \approx \frac{G_0}{G_L}, \tag{53}$$

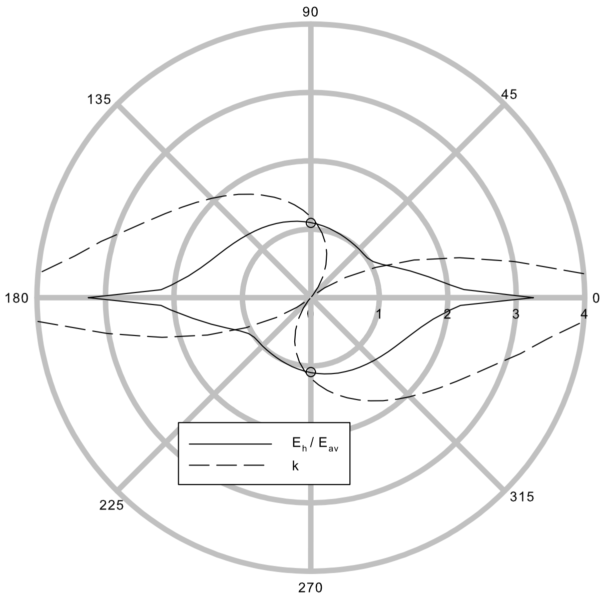

Fig. 3 The *solid* and *dashed lines* show the behavior of the optimal value of E_h/E_{av} and k respectively, as the parameter t in (45) is varied. The values $\beta = 2$ and $\nu = 1/2$ are used. For hydrostatic loading $E_h = E_{av}$ and $k = 0$, and for an internally pressurized cylinder $E_h/E_{av} = 3.25$ as given in (52) as $k \to \infty$. When the cylinder is externally loaded, the symbols ∘ show the effective stiffness that is found by setting $k = 1/\ln(2)$

where G_L is equal to G_k evaluated when $k = 1/m$.

To illustrate these considerations, consider a cylinder again having the typical values $\beta = 2$ and $\nu = 1/2$. The ratio $\mathcal{I}/\mathcal{O}$ is changed and Fig. 3 shows a polar plot that describes the behavior of E_h/E_{av} and k as the parameter t is varied. When $t = 0$ the ratio $E_h/E_{av} = 3.25$ as given in (52), when $t = 45^\circ$ the effective stiffness $E_h = E_{av}$ corresponds to $k = 0$, and when $t = 90^\circ$, setting $k = 1/\ln(2) \approx 1.44$ gives a reasonable estimate as shown by the ∘ symbols.

8 Effect of Spatially Varying Poisson's Ratio

In the preceding analysis Poisson's ratio has been held fixed and $\mathtt{E}$ has been allowed to vary. The case where both E and ν are allowed to vary has been previously treated [14, 15]; here the special case is considered where the stiffness is held constant, i.e., $\mathtt{E} = 1$, and Poisson's ratio is allowed to vary. If $\mathtt{E}$ is held constant, then (13) is written as $\rho^2\psi'' + \rho\psi' - \psi(1 + \rho\nu') = 0$. If ν is then assigned the form $\nu = c_o + c_1 \ln\rho$, then this differential equation reduces to a Cauchy type and the solution is readily obtained. Suppose that ν_a and ν_b represent values of Poisson's ratio at the inner and outer surfaces respectively. These boundary values are satisfied by setting $\nu = \nu_a + c\ln\rho$ where $c = (\nu_b - \nu_a)/\ln\beta$. The stress function that satisfies the boundary conditions in (12) is given by

$$\psi = \left(\frac{\mathcal{O}\beta - \mathcal{I}/\beta^s}{\beta^s - 1/\beta^s}\right)\rho^s + \left(\frac{\mathcal{I}\beta^s - \mathcal{O}\beta}{\beta^s - 1/\beta^s}\right)\frac{1}{\rho^s}, \tag{54}$$

where $s = \sqrt{1+c}$. The integral G in (18) is then calculated

$$G(\nu_a, \nu_b) = \frac{1}{2}\big[\mathcal{I}^2(s\operatorname{cth} sm + \nu_a) - 2\mathcal{O}\mathcal{I}\exp[m]s\operatorname{csch} sm + \mathcal{O}^2\exp[2m](s\operatorname{cth} sm - \nu_b)\big]. \tag{55}$$

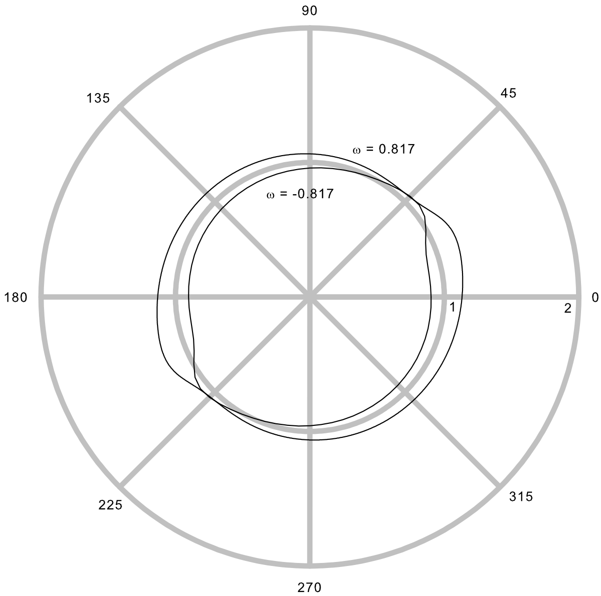

Fig. 4 Polar graph showing the behavior of E_h/E_{av} (the length from the origin to a point on the curve) versus the load parameter t given in (45). Values $\beta = 2$ and $\nu_{av} = 1/2$ are used and the *two lines* show the behavior of E_h/E_{av} when $\mathtt{E} = 1$ and $\omega = \pm 0.817$ as indicated

This expression is valid for both real and imaginary values of s, and if $s = 1$ then the expression reduces to G_0, given in (41), which represents a homogeneous solid.

Proceeding in the same vein as previously described, for a given average value ν_{av} we want to investigate how the spatial dependence of ν affects the overall equivalent stiffness. The average value, ν_{av}, is written as

$$\nu_{av} = \nu_a + (\nu_b - \nu_a) f, \tag{56}$$

where

$$f = \frac{\beta^2}{\beta^2 - 1} - \frac{1}{2 \ln \beta}.$$

The effective modulus $E_h/E_{av} = G(\nu_{av}, \nu_{av})/G(\nu_a, \nu_b)$ is written as

$$\frac{E_h}{E_{av}} = \frac{\mathcal{I}^2(\operatorname{cth} m + \nu_{av}) - 2\mathcal{O}\mathcal{I} \exp[m] \operatorname{csch} m + \mathcal{O}^2 \exp[2m](\operatorname{cth} m - \nu_{av})}{\mathcal{I}^2(s \operatorname{cth} sm + \nu_a) - 2\mathcal{O}\mathcal{I} \exp[m] s \operatorname{csch} sm + \mathcal{O}^2 \exp[2m](s \operatorname{cth} sm - \nu_b)}. \tag{57}$$

Across the wall thickness the change in Poisson's ratio is $\omega = \nu_b - \nu_a = (\nu_{av} - \nu_a)/f$ and this result follows from (56). For comparison with previous results we set $\nu_{av} = 1/2$ and $\beta = 2$ so that $f \approx 0.612$. If $\nu_a = 0$ it follows that $\omega = 1/2f \approx 0.817$ and $\nu_b = \omega$. If $\nu_a = 1$ then $\omega = -1/2f \approx -0.817$ and $\nu_b = \nu_a + \omega \approx 0.183$. Fig. 4 shows the behavior of E_h/E_{av} and it appears that E_h is larger when $\nu_b > \nu_a$ corresponding to $\omega > 0$. The maximum difference of about 25 % between the two cases occurs when $t = 0$, corresponding to internal pressure.

9 Remarks

The homogenization of material moduli of a heterogeneous solid plays a significant role in structural analysis. The analysis of boundary-value problems for an energetically equivalent homogeneous cylinder will enable engineers to quickly decide which cylinders will have the least overall strain energy of deformation which sometimes is taken as the design criterion. One can then analyze in detail the problem for the corresponding inhomogeneous cylinder and ascertain stress singularities at points adjacent to the inclusions/matrix interfaces.

10 Conclusions

We have studied the axisymmetric plane strain deformations of a FG circular cylinder with uniform pressures applied on the inner and the outer surfaces. The goal has been to find the stiffness, E_h, of an energetically equivalent homogeneous cylinder. This paper has three main contributions:

1. For a power law variation of E it is found that the upper and lower bounds of E_h calculated by using two series terms, are reasonably close to the analytical values of E_h. In general, the Voigt and Reuss bounds are not valid.
2. The spatial variation of the stiffness that maximizes the equivalent modulus E_h has been estimated when Poisson's ratio is constant. It has been found that the radial distribution of E, that leads to the maximum value of E_h, depends upon the ratio of internal to external pressure. For pressure applied at the inner surface, E_h is largest when the stiffness is increased near the inner surface. For equal pressures applied on the inner and the outer surfaces of a cylinder E_h has the maximum value for a homogeneous cylinder. For pressure applied at the outer surface, the value E_h is largest when $k \approx 1/\ln \beta$.
3. The effect of spatial variation of Poisson's ratio that increases the equivalent modulus E_h has been considered when the stiffness is constant. The equivalent stiffness, E_h is increased when Poisson's ratio is large near the outer surface.

It is hoped that these observations will be useful in the design of FG cylinders to optimize their elastic properties.

Acknowledgements Funding for Dryden was provided by NSERC, and for Batra by ONR grant N00014-11-1-0594.

References

1. Timoshenko, S., Goodier, J.N.: Theory of Elasticity, 3rd edn. McGraw-Hill, New York (1970)
2. Sokolnikoff, I.S.: Mathematical Theory of Elasticity. McGraw-Hill, New York (1956)
3. Wang, C.: Applied Elasticity. McGraw-Hill, New York (1953)
4. Muskhelishvili, N.I.: Some Basic Problems of the Mathematical Theory of Elasticity, 4th edn. Noordhoff, Groningen (1963)
5. Jabbari, M., Sohrabpour, S., Eslami, M.R.: Mechanical and thermal stresses in a functionally graded hollow cylinder due to radially symmetric loads. Int. J. Press. Vessels Piping **79**, 493–497 (2002)
6. Fettahlioglu, O.A., Steele, T.K.: Thermal deformations and stresses in circularly curved thin beams and rings. J. Therm. Stresses **11**(3), 233–255 (1988)
7. Mohammadi, M., Dryden, J.R.: Thermal stresses in a nonhomogeneous curved beam. J. Therm. Stresses **31**, 587–598 (2008)
8. Jabbari, M., Sohrabpour, S., Eslami, M.R.: General solutions for mechanical and thermal stresses in a functionally graded hollow cylinder due to nonaxisymmetric steady-state loads. J. Appl. Mech., Trans. ASME **70**, 111–118 (2003)
9. Tarn, J.Q.: Exact solutions for functionally graded anisotropic cylinders subjected to thermal and mechanical loads. Int. J. Solids Struct. **38**, 8189–8206 (2001)
10. Zimmerman, R.W., Lutz, M.P.: Thermal stresses and thermal expansion in a uniformly heated functionally graded cylinder. J. Therm. Stresses **22**, 177–188 (1999)

11. Lutz, M.P., Zimmerman, R.W.: Thermal stresses and effective thermal expansion coefficient of a functionally gradient sphere. J. Therm. Stresses **19**, 39–54 (1996)
12. Shao, Z.S., Wang, T.J.: Three-dimensional solutions for the stress fields in functionally graded cylindrical panel with finite length and subjected to thermal/mechanical loads. Int. J. Solids Struct. **43**, 3856–3874 (2006)
13. Tutuncu, N.: Stresses in thick-walled FGM cylinders with exponentially-varying properties. Eng. Struct. **29**, 2032–2035 (2007)
14. Mohammadi, M., Dryden, J.R.: Influence of the spatial variation of Poisson's ratio upon the elastic field in nonhomogeneous axisymmetric bodies. Int. J. Solids Struct. **46**, 788–795 (2009)
15. Nie, G.J., Batra, R.C.: Exact solutions and material tailoring for functionally graded hollow circular cylinders. J. Elast. **99**(2), 179–201 (2010)
16. Nie, G.J., Batra, R.C.: Material tailoring and analysis of functionally graded isotropic and incompressible linear elastic hollow cylinders. Compos. Struct. **92**, 265–274 (2010)
17. Dryden, J., Jayaraman, K.: Effect of inhomogeneity on the stress in pipes. J. Elast. **83**, 179–189 (2006)
18. Theotokoglou, E.E., Stampouloglou, I.H.: The radially nonhomogeneous elastic axisymmetric problem. Int. J. Solids Struct. **45**, 6535–6552 (2008)
19. Rooney, F.J., Ferrari, M.: Torsion and flexure of inhomogeneous elements. Compos. Eng. **5**(7), 901–911 (2003)
20. Genin, G.M., Birman, V.: Micromechanics and structural response of functionally graded, particulatematrix, fiber-reinforced composites. Int. J. Solids Struct. **46**, 2136–2150 (2009)
21. Lekhnitskii, S.G.: Theory of Elasticity of an Anisotropic Body. Mir, Moscow (1981)
22. Pan, E., Roy, A.K.: A simple plane-strain solution for functionally graded multilayered isotropic cylinders. Struct. Eng. Mech. **24**(6), 727–740 (2006)
23. Horgan, C.O., Chan, A.M.: The pressurized hollow cylinder or disk problem for functionally graded isotropic linearly elastic materials. J. Elast. **55**, 43–59 (1999)
24. Oral, A., Anlas, G.: Effects of radially varying moduli on stress distribution of nonhomogeneous anisotropic cylindrical bodies. Int. J. Solids Struct. **38**(20), 5568–5588 (2005)
25. Chen, Y.Z., Lin, X.Y.: Elastic analysis for thick cylinders and spherical pressure vessels made of functionally graded materials. Comput. Mater. Sci. **44**, 581–587 (2008)
26. Li, X.F., Peng, X.L.: A pressurized functionally graded hollow cylinder with arbitrarily varying material properties. J. Elast. **96**, 81–95 (2009)
27. Batra, R.C.: Optimal design of functionally graded incompressible linear elastic cylinders and spheres. AIAA J. **46**(8), 2050–2057 (2010)
28. Gal, D., Dvorkin, J.: Stresses in anisotropic cylinders. Mech. Res. Commun. **22**, 109–113 (1995)
29. Lutz, M.P., Zimmerman, R.W.: Effect of the interphase zone on the bulk modulus of a particulate composite. J. Appl. Mech., Trans. ASME **63**, 855–861 (1996)
30. Markworth, A.J., Ramesh, K.S., Parks, W.P.: Modelling studies applied to functionally graded materials. J. Mater. Sci. **30**, 2183–2193 (1995)
31. Birman, V., Byrd, L.W.: Modeling and analysis of functionally graded materials and structure. Appl. Mech. Rev. **60**, 195–216 (2007)
32. Subbaraman, G., Reifsnider, K.L.: Mechanical response of fuel clad with radial property variations. In: 12th Annual. Mtg. SES, University of Texas, vol. 36, pp. 1235–1247 (1976)
33. Francfort, G.A., Murat, F.: Homogenization and optimal bounds in linear elasticity. Arch. Ration. Mech. Anal. **94**(4), 307–334 (1986)
34. Paul, B.: Prediction of elastic constants of multiphase materials. Trans. Metall. Soc. AIME **218**, 36–41 (1960)
35. Mura, T.: Micromechanics of Defects in Solids, 2nd edn. Martinus Nijhoff, Boston (1987)
36. Torquanto, S.: Random Heterogeneous Materials. Springer, New York (2002)
37. Cherkaev, A.: Variational Methods for Structural Optimization. Springer, New York (2000)
38. Avseth, P., Mukerji, T., Mavko, G.: Quantitative Seismic Interpretation: Applying Rock Physics Tools to Reduce Interpretation Risk. Cambridge University Press, Cambridge (2005)
39. Arthurs, A.M.: Complementary Variational Principles. Clarendon, Oxford (1980)